

This article was downloaded by:

On: 30 January 2011

Access details: Access Details: Free Access

Publisher Taylor & Francis

Informa Ltd Registered in England and Wales Registered Number: 1072954 Registered office: Mortimer House, 37-41 Mortimer Street, London W1T 3JH, UK



Spectroscopy Letters

Publication details, including instructions for authors and subscription information:

<http://www.informaworld.com/smpp/title~content=t713597299>

Electronic Spectra and High-Resolution B-type Delayed Fluorescence of Salicylidene-*m*-bromo-aniline in Hexane

Fuat Bayrakçeken^a; Haluk Küçük^b

^a Department of Biomedical Engineering, Yeditepe University, Division of Optical Spectroscopy, Istanbul, Turkey ^b Department of Mechatronics Education, Marmara University, Istanbul, Turkey

To cite this Article Bayrakçeken, Fuat and Küçük, Haluk(2009) 'Electronic Spectra and High-Resolution B-type Delayed Fluorescence of Salicylidene-*m*-bromo-aniline in Hexane', Spectroscopy Letters, 42: 2, 87 — 94

To link to this Article: DOI: 10.1080/00387010802428641

URL: <http://dx.doi.org/10.1080/00387010802428641>

PLEASE SCROLL DOWN FOR ARTICLE

Full terms and conditions of use: <http://www.informaworld.com/terms-and-conditions-of-access.pdf>

This article may be used for research, teaching and private study purposes. Any substantial or systematic reproduction, re-distribution, re-selling, loan or sub-licensing, systematic supply or distribution in any form to anyone is expressly forbidden.

The publisher does not give any warranty express or implied or make any representation that the contents will be complete or accurate or up to date. The accuracy of any instructions, formulae and drug doses should be independently verified with primary sources. The publisher shall not be liable for any loss, actions, claims, proceedings, demand or costs or damages whatsoever or howsoever caused arising directly or indirectly in connection with or arising out of the use of this material.

Electronic Spectra and High-Resolution B-type Delayed Fluorescence of Salicylidene-*m*-bromo-aniline in Hexane

Fuat Bayrakçeken¹,
and Haluk Küçük²

¹Yeditepe University, Division of Optical Spectroscopy, Department of Biomedical Engineering, Istanbul, Turkey

²Marmara University, Department of Mechatronics Education, Istanbul, Turkey

ABSTRACT The observation of triplet–triplet absorption and emissions of salicylidene-*m*-bromo-aniline is complicated by possible colored isomer formation during the optical pumping. The short-lived (singlet–singlet) and long-lived (triplet–triplet) absorption spectra were recorded photographically by microsecond flash and nanosecond laser flash photolysis techniques. Salicylidene–aniline complexes were purified by repeated recrystallization until further recrystallization produced no further changes for X-ray diffraction pattern and optical absorption emission properties. B-type delayed fluorescence, T-T absorption, color isomer absorption, and T-T emissions of this compound were recorded for the first time.

KEYWORDS activation energy, B-type delayed fluorescence, entropy change, salicylidene-*m*-bromo-aniline, T-T absorption, T-T fluorescence

INTRODUCTION

In the crystalline state, salicylidene–aniline and its derivatives (called anils) undergo reversible color changes induced by ultraviolet light or heat. The color change process can be reversed by using different optical pumping bands, therefore bleaching occurs. Any one anil crystalline form can be either photochromic or thermochromic, but not both. In rigid solutions, these compounds are photochromic, and photochromism is an intrinsic property of the individual anil molecule rather than a result of molecular interactions in the crystals. The hydroxyl group in an ortho position was considered an essential condition for this phenomenon, and it was proposed that the action of light upon the anils causes a hydrogen atom transfer to form a keto anil.

Using flash photolysis technique, $S_0 \rightarrow S_n$ absorption bands below 380 nm and relatively weak $T_1 \rightarrow T_n$ absorption band between 410 nm and 450 nm were found. The photoproduct color isomer absorbs strongly below 555 nm, as seen in Fig. 1. Absorption of light by a molecule results in the formation of an excited state. This state can be deactivated by either a photophysical process or a photochemical process like dissociation into free radicals or ionization. In most cases though practically most of the energy is

Received 18 April 2008;
accepted 29 July 2008.

Address correspondence to Fuat Bayrakçeken, Yeditepe University, Division of Optical Spectroscopy, Department of Biomedical Engineering, 34755, Istanbul, Turkey.
E-mail: fubay@yeditepe.edu.tr

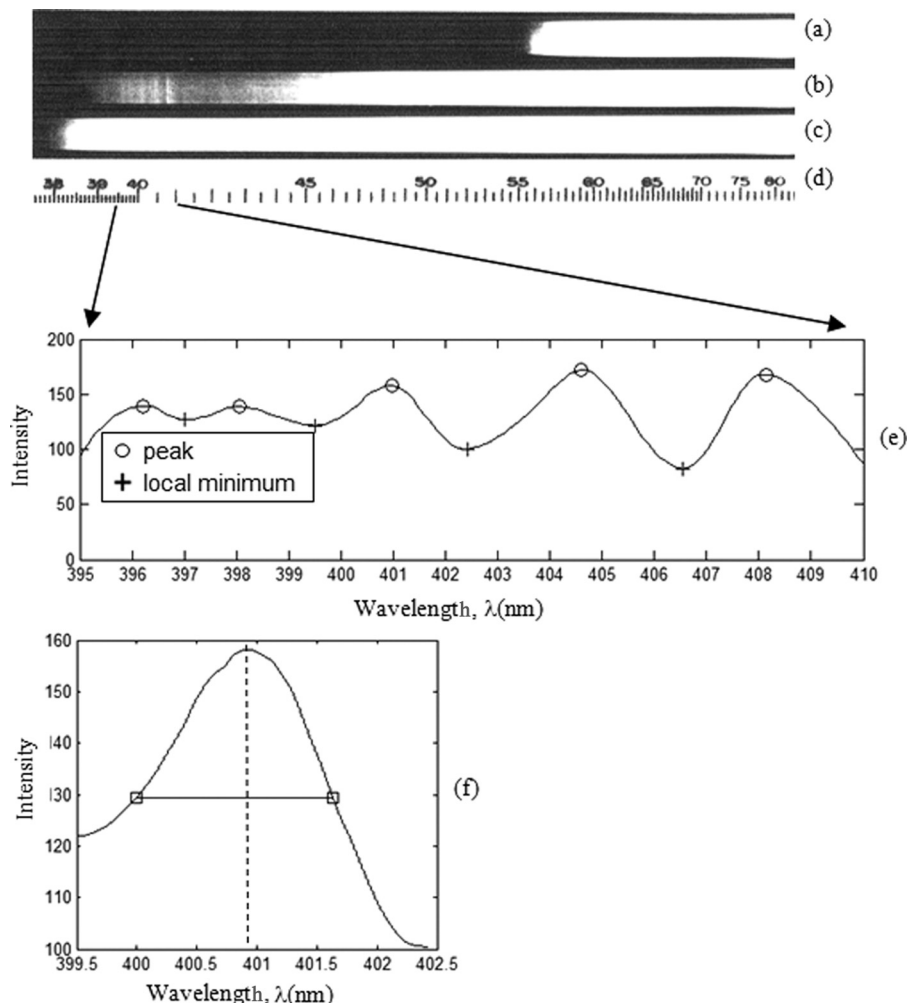


FIGURE 1 (a) Photoproduct (color isomer) absorption spectrum of salicylidene-*m*-bromo-aniline in hexane at room temperature. (b) $T_1 \rightarrow T_n$ absorption spectrum and high-resolution B-type delayed fluorescence of salicylidene-*m*-bromo-aniline in hexane at room temperature. (c) $S_1 \rightarrow S_0$ absorption of salicylidene-*m*-bromo-aniline in hexane at room temperature. (d) Wavelength scale, 380-800 nm. (e) B-type delayed fluorescence spectrum of salicylidene-*m*-bromo-aniline in hexane at room temperature. (f) First fluorescence line shape (0-0 transition) and bandwidth of salicylidene-*m*-bromo-aniline in hexane at room temperature.

lost by a photophysical process, a definite action of exciting energy results in neutral radical or ion-radical formation. The photolytic method is often a good way of producing specific radicals, as one can irradiate with light of energy capable of breaking only the required bond.

The tautomerism has recently been evidenced by X-ray diffraction as a dynamic disorder in crystals. Most salicylidene-anilines including the parent compound greatly favor the "OH" form in both crystal and solutions. However, it has been noted that if a nitro group is introduced into the benzene ring of the salicylaldehyde part, the tautomeric behavior is changed significantly. The crystal structure does not show any van der Waals contact or intermolecular hydrogen bonding. The most stable conformation

of the "NH" form is nearly planar. The destabilization energy is estimated between the planar and the twisted "OH" form. Thus the energy difference between the "OH" and "NH" forms is considerably smaller in the crystals than in the solution.^[1-41]

MATERIALS AND METHODS

All the chemicals used were spectroscopically pure, Aldrich grade, and used as received without further purifications. Anils were prepared by warming equimolar quantities of *m*-bromo-aniline and salicylaldehyde in hexane and allowing the solution to cool. This compound crystallized as yellow granules. Orange crystals were obtained by crystallization from ethanol or *n*-heptane below 6°C. These crystals were

not photochromic but fluoresced strongly under 365 nm radiation; this variety is called the β -form of the anilines. The solutions were prepared in “low activity” flasks in order to prevent any photo conversion by room light and were allowed to stand in the dark overnight before the experiments. Then the solution was placed into a 20-cm-long, double-walled quartz vessel, which has optically flat end windows and with a surrounding outer jacket containing a liquid filter (0.75 g iodine in 100 mL, CCl_4) 1 cm in thickness. Temperature gradients in the cell were avoided by circulating the filter solution through a thermostated bath by means of an all-glass system through the reaction vessel’s outer jacket to act as an ultraviolet cutoff filter and to thermostat the sample in the temperature range 10–60°C. $\text{S}_0 \rightarrow \text{S}_n$ absorption spectrum was recorded by a Perkin-Elmer Lambda 2 UV-vis spectrophotometer (Perkin-Elmer, Waltham, Massachusetts, USA) at room temperature, and T-T absorption spectrum of the title compound was recorded by a Hilger medium quartz spectrograph, London, England (slitwidth 0.025 nm). Ilford HP-3 plates were used and were developed in Ilford PQ universal developer. The flash photolysis apparatus employed two air-filled photolysis lamps in series, with a flash duration of 2 μs . An electrical energy of approximately 1125 J (10 μF , 15 kV) was discharged through the air-filled flash lamps. In order to get rid of the stray light, the ends of the reaction cell were shielded with blackened light hoods.

The original image of the multiresolution spectra was scanned by a RexRotary scanner (USA) at 600 dpi resolution to obtain a high-resolution digital image. The original spectrum image was transformed to gray level image and normalized by using MATLAB functions. The contrast of the image was enhanced by transforming the values using contrast-limited adaptive histogram equalization (CLAHE). CLAHE operates on small regions in the image, called tiles, rather than on the entire image. Each tile’s contrast is enhanced, so that the histogram of the output region approximately matches the histogram specified by the “Distribution” parameter. The neighboring tiles are then combined using bilinear interpolation to eliminate artificially induced boundaries. The contrast, especially in homogeneous areas, can be limited to avoid amplifying any noise that might be present in the image. One-dimensional

TABLE 1 Location of the B-type Delayed Fluorescence Lines in the Ultraviolet (All Kinds of Fluorescence Observed at the Same Band)

| Peak location (nm) | Peak height (intensity) | Half bandwidth (nm) | Photoproduct color isomer |
|--------------------|-------------------------|---------------------|-----------------------------------|
| 396.2097 | 139.5184 | 2.1590 | $\Delta\lambda_a = 200$ to 555 nm |
| 398.0645 | 138.9817 | 1.2873 | |
| 400.9677 | 158.0521 | 1.6428 | |
| 404.5968 | 172.2874 | 2.1028 | |
| 408.1452 | 167.8936 | 2.0294 | |

density information of emission bands was extracted by computing the averages of the rows through vertical axes. A MATLAB smoothing based on rloess (robust local polynomial regression), the robust version of loess (local polynomial regression) method, was applied to the computed density curves to reduce the noise effect on the densities. The loess method is based on local regression using weighted linear least squares and a second degree polynomial model. The robust version of loess assigns lower weight to outliers in the regression. The method assigns zero weight to data outside six mean absolute deviations. Figure 1 shows the experimentally recorded absorption spectra of bands (a), (b), (c), computed in one-dimensional densities, and corresponding scale positions in Fig. 1 (e) and (f). Each density curve having a maximum level between the points marked as local minimum was defined as an absorption band on the spectra. Then each band was separated from the density data and plotted again to determine the half bandwidth. The half of the difference between the maximum level of the band and the lowest of the local minimums surrounding the band is measured to determine location of the horizontal line for calculation of half bandwidth. Table 1 shows the half bandwidth and the band peak level and corresponding location of the data.

RESULTS AND DISCUSSION

The sample salicylidene-*m*-bromo-aniline solutions of 3.5×10^{-4} molar concentration were flashed at different temperatures between room temperature and 50°C and at -74°C.

The concentrations were chosen as the lowest convenient value for which the resulting concentrations of triplet-triplet absorption species gave

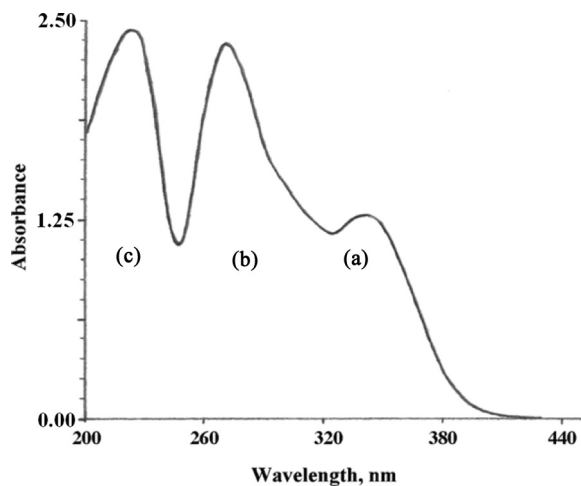


FIGURE 2 $S_0 \rightarrow S_n$ absorption spectrum of salicylidene-*m*-bromo-aniline in hexane at room temperature. (a) $S_0 \rightarrow S_1$ absorption band; (b) $S_0 \rightarrow S_2$ absorption band; (c) $S_0 \rightarrow S_3$ absorption band.

enough contrast on the photographic plate. Photographic plates were extrasensitized by sodium salicylate to get better contrast for the high-resolution B-type delayed fluorescence band between 390 and 410 nm region.

The decay kinetic energy was first order, therefore, long-lived photoproducts were not observed as absorption or emission bands on the spectrum.

A quite simple way of differentiating between radical and triplet state absorptions occurring in flash photolysis and laser flash photolysis is to compare the spectra observed in the presence and absence of air. Because the rate of quenching triplet states by paramagnetic oxygen is so fast, no triplet state absorption is seen in the presence of air, whereas

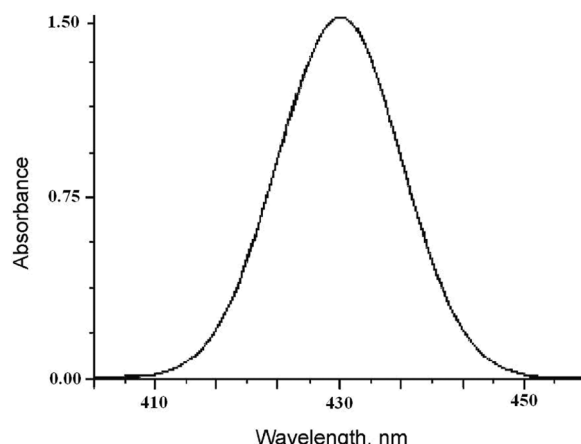


FIGURE 3 Background subtracted $T_1 \rightarrow T_n$ absorption spectrum of salicylidene-*m*-bromo-aniline in hexane at room temperature.

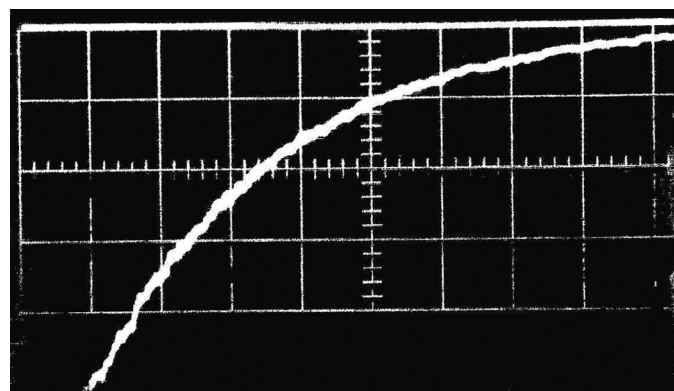


FIGURE 4 B-type delayed fluorescence decay of salicylidene-*m*-bromo-aniline in hexane at room temperature. Vertical, 1 V/full scale; horizontal, 1 ms/cm. $\lambda_{ex} = 330$ nm $S_0 \rightarrow S_1$ absorption band, $\lambda_e = 390$ to 410 nm $T_2 \rightarrow S_1 \rightarrow S_0$; B-type delayed fluorescence (emission via S_1 state) $\tau_{1/e}$ (B-type) = 0.25 ± 0.10 μ s.

both radical and triplet state absorptions are seen in the absence of air. This method depends on the fact that in general, aromatic radicals react rather slowly with oxygen, but it is only suitable when the presence of air does not interfere with photolytic formation of triplet states and radicals. Figure 1 shows the $S_0 \rightarrow S_1$, $T_1 \rightarrow T_n$, and color isomer absorption band, and high-resolution B-type delayed fluorescence of the title compound in hexane at room temperature, recorded by microsecond flash photolysis apparatus, and Figure 2 shows the $S_0 \rightarrow S_n$ absorption bands recorded by a steady state, UV-vis spectrophotometer; high-resolution B-type delayed fluorescence and $T_1 \rightarrow T_n$ absorption bands were recorded photographically by flash photolysis technique. Figure 3, shows the background subtracted triplet-triplet absorption spectrum of salicylidene-*m*-bromo-aniline in hexane at room

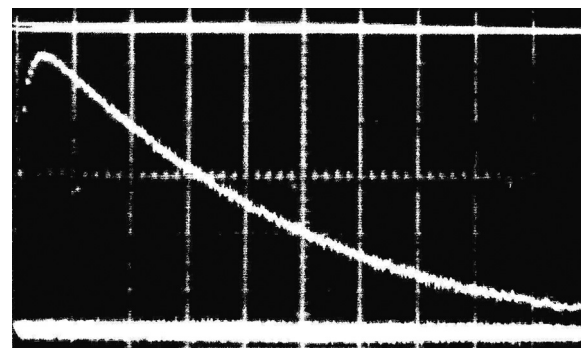


FIGURE 5 T_1 decay of salicylidene-*m*-bromo-aniline in hexane at room temperature. Disappearance of T_1 ; vertical, 1 V/full scale; horizontal, 1 ms/cm. $\lambda_{ex} = 430$ nm, $\lambda_{decay} = 440$ nm, $\tau_{1/e}$ (disappearance of T_1 state) = 5.0 ± 0.5 ms.

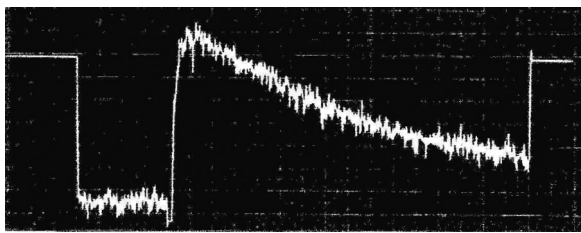


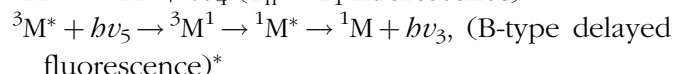
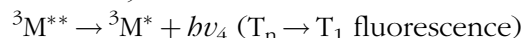
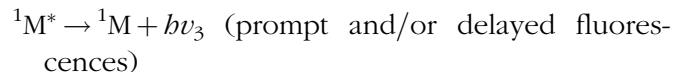
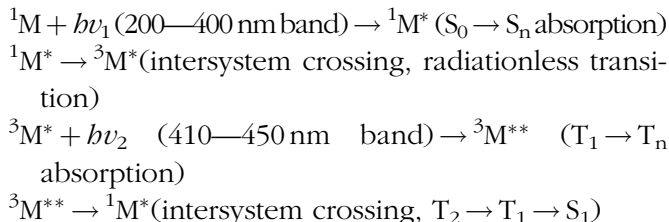
FIGURE 6 T_1 decay of salicylidene-*m*-bromo-aniline in hexane at -74°C . Disappearance of T_1 state concentration, population; vertical, 2 V/full scale; horizontal, 1 ms/division. $\lambda_{\text{ex}} = 430\text{ nm}$, $\lambda_{\text{decay}} = 440\text{ nm}$, $\tau_{1/e}$ (disappearance of T_1 state) = $13.0 \pm 1.0\text{ ms}$.

temperature; the peak observed at 430 nm with half-bandwidth 20.21 nm B-type delayed fluorescence was observed strongly between 390 and 410 nm band as discrete line.^[21]

Figure 4 shows B-type delayed fluorescence (disappearance of T_2 state), decay of salicylidene-*m*-bromo-aniline in hexane at room temperature, Figure 5 shows T_1 state decay (disappearance of T_1 population) of the title compound, and Figure 6 shows T_1 state decay (disappearance of T_1 state) at -74°C . Table 2 shows spectroscopic parameters of the title compound.

Reaction Mechanism

The photophysical mechanism of the reaction is as follows:



The rate constant k and the entropy change ΔS^* were obtained using the following formula:

$$k = (e) \cdot \left(\frac{kT}{b} \right) \cdot (e^{-E_{\text{exp}}/RT}) \cdot (e^{\Delta S^*/R}).$$

Energy of activation and entropy change were found to be +7.95 kcal/mole and -16.47 e.u. , respectively, for salicylidene-*m*-bromo-aniline in hexane at room temperature.

Although it was not observed for the title compound experimentally, there is always a possibility to see the excimer fluorescence, which will appear at longer wavelengths than will normal fluorescence.

In this particular case, the reaction mechanism will be

$^1\text{M}^*$ = Molecule is the first electronically excited state

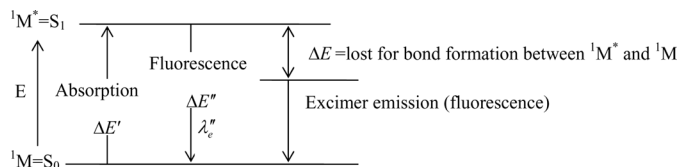
^1M = Molecule is the ground state electronic level, therefore we can write

$^1\text{M}^* + ^1\text{M} \xrightarrow{\text{collision}} (\text{M} \dots \text{M}^*)$ = excimer (bond formed); for this reason, some energy is taken from the first electronically excited state of the molecule.

Fluorescence wavelengths of the excimer will appear at longer wavelengths than will normal fluorescence.

TABLE 2 Absorption and Emission Parameters of Salicylidene-*m*-bromo-aniline in Hexane at Room temperature

| $\text{S}_0 \rightarrow \text{S}_n$ absorptions peak locations (nm) | $\text{S}_1 \rightarrow \text{S}_0$ emission (nm) | $\text{T}_1 \rightarrow \text{T}_n$ absorption | $\tau_{1/e}(\text{T}_2)$ disappearance of T_2 state | $\tau_{1/e}(\text{T}_1)$ disappearance of T_1 state concentration, population |
|--|---|---|---|---|
| 330 | 396 | $\Delta\lambda_d = 410$ to 450 nm | B-type | T_1 triplet |
| 270 | 401 | band peak | delayed fluorescence | $\text{decay} = 5.0 \pm 0.5\text{ ms}$ |
| 220 | 404 | $\lambda_{\text{max}} = 430\text{ nm}$ | emission band | at 25°C |
| $\Delta\lambda_d = 200$ to 420 nm band | 405 | at peak | 396 to 408 nm | $\text{decay} = 13 \pm 1.0\text{ ms}$ |
| | 407 | | band $\tau_{1/e} = 0.25 \pm 0.10\text{ }\mu\text{s}$ | at -74°C |
| | | $\Delta\lambda_d = 396$ to 407 nm band | | |



Here, $\Delta E' > \Delta E'' > \Delta E^*$, therefore excimer emissions appeared at longer wavelengths than did normal fluorescence. There is no possibility to see exciplex emissions, because there is only one type of molecule in the reaction cell. Formation of exciplex between solute and solvent has never been observed in flash spectroscopy in the optical bands.

CONCLUSIONS

If the medium is optically dense, the phenomenon known as radiation trapping may play a significant role. An emitted photon from S_1 state can be absorbed by another molecule in the reaction cell instead of escaping from the medium. The lifetime increase due to radiation trapping depends on the molecular density, on the cross section of the transition involved, and on the geometry of the system. The emission may take place by a cooperative process in which the emission of one molecule is influenced by the emission of the others. This leads to the phenomena of superradiance and superfluorescence. We used rod-shaped active material in solution, therefore, molecular concentration is even inside the reaction cell. For a rod-shaped active material, with diameter D , the light will be emitted into a solid angle corresponding with the diffraction angle $\theta_d = \lambda/D$; the peak power of the B-type delayed fluorescence now varies as (NV^2) , where N is the critical inversion and $V = \pi D^2 L/4$ is the critical volume rather than NV , as would be the case for the normal emission process. If the system emits normal and delayed fluorescences at different decay times but in the same emission band, the fluorescence will appear as discrete lines instead of a broad fluorescence band on the photographic plate. The intensity of the superfluorescence is higher in intensity than the normal fluorescence because of the radiation trapping. If the fraction of molecules initially in the upper state is such that population inversion occurs, emission of the molecule is influenced by the emission of the others. This leads to the superfluorescence. This phenomenon is only observed for gas

or vapor phase flash photolysis experiments and rarely in dilute solutions because density is constant everywhere in the reaction cell. Active material was rod-shaped and the photolysis lamps were also rod-shaped, which are placed in a cylindrical shape cavity. The cavity was coated by front surface mirror to get the maximum number of photons (in this experiment, number of photons = 10^8 /pulse).

B-type delayed fluorescence discrete lines showed that neither phantom triplet nor twisted triplet states were formed during the pulse optical pumping. All kinds of energy transfers were optical in nature. Discrete emission lines did not belong to the emission lines of photolysis or spectral flash lamps. T-T absorption is a Gaussian type and very symmetrical around the peak location, therefore, we can say that these emitted lines (B-type delayed fluorescence) have to be coherent emissions. This material can be used as an optical sensor for sensor physics applications.

If the molecule interacts with photons at different frequencies at a very high photon flux, yotta-photon (10^{24} photon/pulse) excitation creates very high photon flux, in other words the molecules interact with light in a photon field, therefore all the transitions up and/or down (i.e., optical, thermal, collisional, photochemical, photophysical) are possible. When radiation (at high photon flux) interacts with molecules, it is useful to consider the response of the molecule to a photon field. Any collection of charged or uncharged particles will respond through its polarization, which may be expanded in increasing powers of photon field P . In high photon flux intensity experiments, electrical field and magnetic fields are also created in the vicinity of the reaction cell in the cavity, therefore light scattering is also possible through the reaction cell. There is no spontaneous emissions for flash photolysis experiments. All are stimulated emissions. There are no molecules or atoms that emit spontaneous emissions. Therefore the system has to be excited in the first step, then emissions can be observed. The excitations can be optical, thermal, collisional, energy transfer, and so on. For this reason, "Einstein coefficients" for spontaneous emissions are imaginary, therefore they are not correct experimentally, because there is no evidence for any system. Unfortunately, these imaginary coefficients are still used in laser or quantum electronics books as real coefficients. When someone writes

a book, generally some parts of the book are taken from reference books. Therefore, the same mistakes are reproduced in the new books. First of all, speaking of a single “speed of light” is incorrect.^[41] There are actually different speeds of propagation for different aspects of a light pulse.

Although the lights emitted from two different sources as pulse or cw (continuous wave) at the same frequency, same amplitude, same phases, and same intensities, the pulsed light and cw light behave physically different. cw polychromatic light interacts with molecules because emission time is infinity, therefore each photon can meet a molecule in the reaction cell during the irradiation time. But for pulsed light, interaction with molecules in the cell is not that simple, because the light in a short time (pulse duration time = $t_r + t_d$) cannot meet a molecule to interact in the reaction cell, although the active medium is rod-shaped.

There are five different kinds of wave velocities: phase, group, energy, signal, and front velocities. As we see from the many scientific books, the speed of light and the velocity of light is taken the same. Which one has the acceleration. Otherwise, faster than light is notpossible. But today many research papers and books explain the faster-than-light systems “superluminal loop holes in physics.” The radiation pressure force is also a factor to increase the speed of light. The destructive interference prevents absorption and causes the molecule to remain in a “dark state,” a coherent superposition of the two ground states. In this article, we have strived to address different concepts in unambiguous terms while remaining true to their wonderfully multifaceted nature. The story of this quest to understand the character of light is a long one indeed and parallels much of the progress of the physical theory. Dual conceptions of light, as wave and particle, have coexisted since antiquity. Each development provides us with fresh insight on the photon question. The particulate nature of the photon is evident in its tendency to be absorbed or emitted by molecules “in discrete units, leading quantization of light energy.” Quantum interference and entanglement are exemplified by one photon and two-photon wave functions, which facilitate comparisons with classic wave optics. Antithetical conceptions of light are its locality as a particle and its functionality as a wave. We all know what the light is, but it is difficult

to explain experimentally what it is. And it will not be easy for another 100 years.^[42]

Einstein did make a surprisingly trivial mistake in introducing the cosmological constant. Although that step made possible a time-independent solution of the Einstein field equations, the solution described a state of unstable equilibrium. The cosmological constant acts like a repulsive force that increases with distance, while the ordinary attractive force of gravitation decreases with distance. Although there is a critical mass density at which this repulsive force just balances the attractive force of gravitation, the balance is unstable; a slight expansion will increase the repulsive force and decrease the attractive force so that the expansion accelerates. It is hard to see how Einstein could have missed this elementary difficulty.

Einstein was also at first confused by an idea he had taken from the philosopher Ernst Mach: that the phenomenon of inertia is caused by distant masses. To keep inertia finite, Einstein in 1917 supposed that the universe must be finite, and so he assumed that its spatial geometry is that of a three-dimensional spherical surface. It was therefore a surprise to him that when test particles are introduced into the empty universe of the Sitter’s model, they exhibit all the usual properties of inertia. In general relativity, the masses of distant bodies are not the cause of inertia, though they do affect the choice of inertial frames. But that mistake was harmless. As Einstein pointed out in his 1917 paper, it was the assumption that the universe is static, not that it is finite, that had made a cosmological constant necessary.

REFERENCES

1. Bayrakçeken, F.; Aktaş, S.; Toptan, M.; Ünlügedik, A. *Spectrochim. Acta A* **2003**, 59, 135.
2. Seymour, E. H.; Lawrence, N. S.; Beckett, E. L.; Davis, J. *Talanta* **2002**, 57, 233.
3. Birkett, H. E.; Cherryman, J. C.; Chippendale, A. M.; Hazendonk, P.; Harris, R. K. *J. Mol. Struct.* **2002**, 59, 602.
4. Bozic, L. T. *Vib. Spectrosc.* **2002**, 28, 235.
5. Taha, A. N.; True, N. *J. Phys. Chem. A* **2000**, 104, 2985.
6. Vasiliev, N. G.; Dimitrov, V. S. *J. Mol. Struct.* **2000**, 522, 37.
7. Estiu, G. L. *J. Mol. Struct.* **1997**, 401, 157.
8. Nagagaki, R.; Aoyama, I.; Chmizu, K.; Akagi, M. *J. Phys. Org. Chem.* **1993**, 6, 261.
9. Sawada, K.; Kanda, T.; Naganuma, Y.; Suzuki, T. *J. Chem. Soc. Dalton Trans.*, **1992**, 2955.
10. Bayrakçeken, F. *METU-J. Pure Appl. Sci.* **1972**, 5(2), 177.
11. Merriman, J. C.; Anthony, D. H. J.; Kraft, J. A.; Wilkinson, R. *J. Chemosphere*, **1991**, 23, 1605.

12. Berjerano, T.; Forgacs, C.; Gileadi, E. *J. Electroanal. Chem.* **1970**, *27*, 469.
13. Lister, D. G.; Tyler, J. K. *J. Chem. Soc. Chem. Commun.* **1996**, *6*, 152.
14. Fukuyo, M.; Hirotsu, K.; Higuchi, T. *Acta Crystallogr. B* **1982**, *38*, 640.
15. Bayrakçeken, F. *Chem. Phys. Lett.* **1980**, *74/2*, 298.
16. Ogawa, K.; Fujiwara, T. *Chem. Lett.* **1999**, *7*, 657.
17. Ogawa, K.; Harada, J.; Tamura, I.; Noda, Y. *Chem Lett.* **2000**, *5*, 528.
18. Cohen, M. D.; Schmidt, G. M. *J. Phys. Chem.* **1962**, *66*, 2442.
19. Ogawa, K.; Harada, J.; Fujiwara, T.; Yoshida, S. *J. Phys. Chem. A* **2001**, *105*, 3425.
20. Bayrakçeken, F. *METU-J. Pure Appl. Sci.* **1978**, *11*(1), 33.
21. Bayrakçeken, F. *J. Lumin.* **1992**, *54*, 29.
22. Bayrakçeken, F.; Topaloğlu, S. *Asian J. Spectrosc.* **2002**, *6*, 77.
23. Zgierski, M. Z.; Grabowska, A. *J. Chem. Phys.* **2000**, *112*(14), 6329.
24. Morales, R. G. E.; Jara, G. P.; Vargas, V. *Spectroscopy Letters* **2001**, *34*(1) 1.
25. Beg, S. A.; Ormson, S. M.; Brown, R. G.; Matousek, P.; Towrie, M.; Nibbering, E. T. J.; Foggi, P.; Neuwahl, F. V. R. *J. Phys. Chem. A* **2001**, *105*, 3709.
26. Shen, M. Y.; Zhao, L. Z.; Goto, T.; Mordiniski, A. *J. Luminescence*, **2000**, *87*(89), 667.
27. Goto, T.; Tashiro, Y. *J. Luminescence*, **1997**, *72*(74), 921.
28. Mitro, S.; Tamai, N. *Chem. Phys. Lett.* **1998**, *282*, 391.
29. Nanoyama, N.; Hisatome, K.; Shoda, C.; Suzuki, H. *Tetrahedron Lett.*, **1999**, *40*, 6939.
30. Bayrakçeken, F. *Spectrochim. Acta A* **2004**, *60*, 923.
31. Karaaslan, I. Ş; Bayrakçeken, F. *Spectrochim. Acta A* **2007**, *68*, 1379.
32. Ha, Y.-Z.; An, J.-Y.; Qin, L.; Jiang, L.-J. *J. Photochem. Photobio. A Chem.*, **1994**, *78*, 247.
33. Previtali, C. M. *J. Photochem. Photobiolo. A Chem.*, **1988**, *41*, 147.
34. VanderDockt, E.; Barthels, M. R.; Delestinne, A. *J. Photochem.* **1973**, *1*, 429.
35. Bayrakçeken, F.; Karaaslan, İ. Ş. *Spectrochimi. Acta A* **2003**, *59*, 2785.
36. Palit, D. K.; Pal, H.; Mukherjee, T.; Mittal, J. P. *J. Photochem. Photobiol. A Chem.* **1988**, *43*, 59.
37. Samanta, A.; Fessenden, R. W. *Chem. Phys. Lett.* **1988**, *153*, 406.
38. Bonnoau, R.; Dubien, J. J.; Bensasson, R. *Chem. Phys. Lett.*, **1969**, *3*, 353.
39. Tagawa, S.; Schnabel, W. *Chem. Phys. Lett.*, **1980**, *75*, 120.
40. Alfassi, Z. B.; Previtali, C. M. *J. Photochem.* **1985**, *30*, 127.
41. Bayrakçeken, F. *Spectrochim. Acta A* **2007**, *68*, 1416.
42. Weinberg, S. *Physics Today* **2005** November issue, 2005, 31.